Earthquake source:

Finite extension
Kinematics
Extended source model

Available observations…

-surface traces (sometimes..)
-geodesy..
-seismograms, accelerograms…


CALIFORNIA
Landers

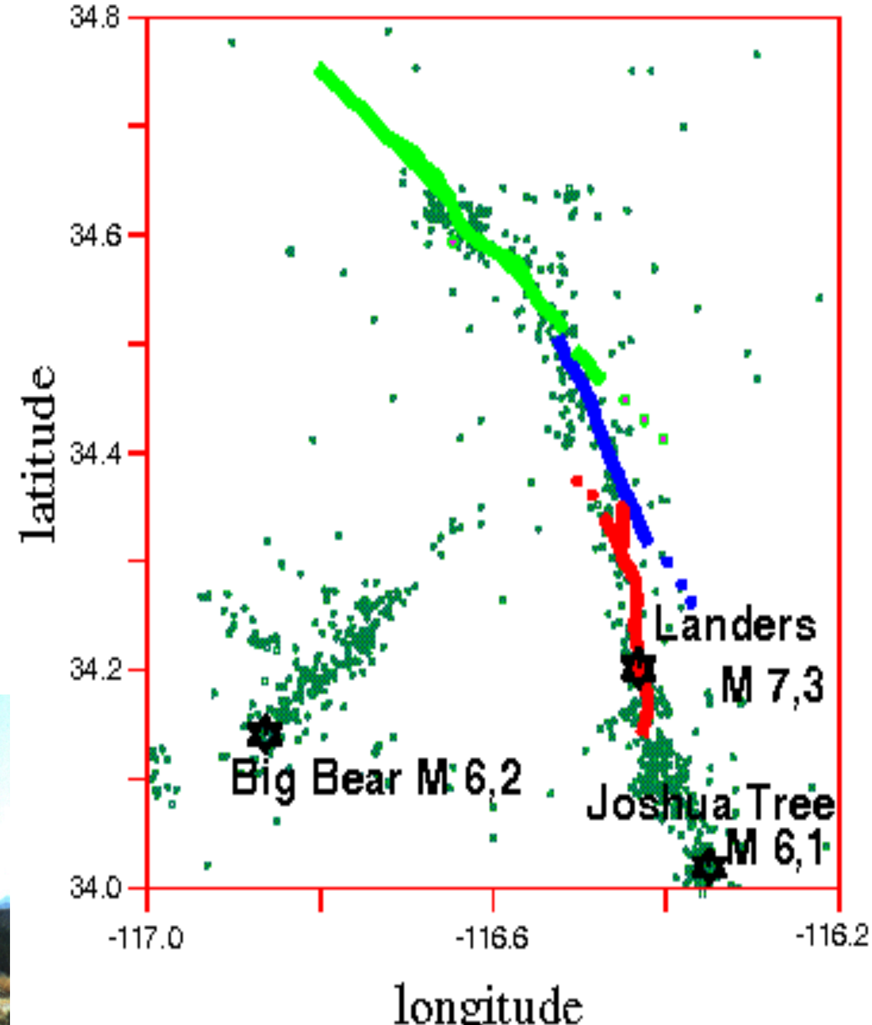
34.8
34.6
34.4
34.2
34.0
latitude
-117.0
-116.6
-116.2
longitude
Landers
M 7,3
Big Bear M 6,2
Joshua Tree
M 6,1

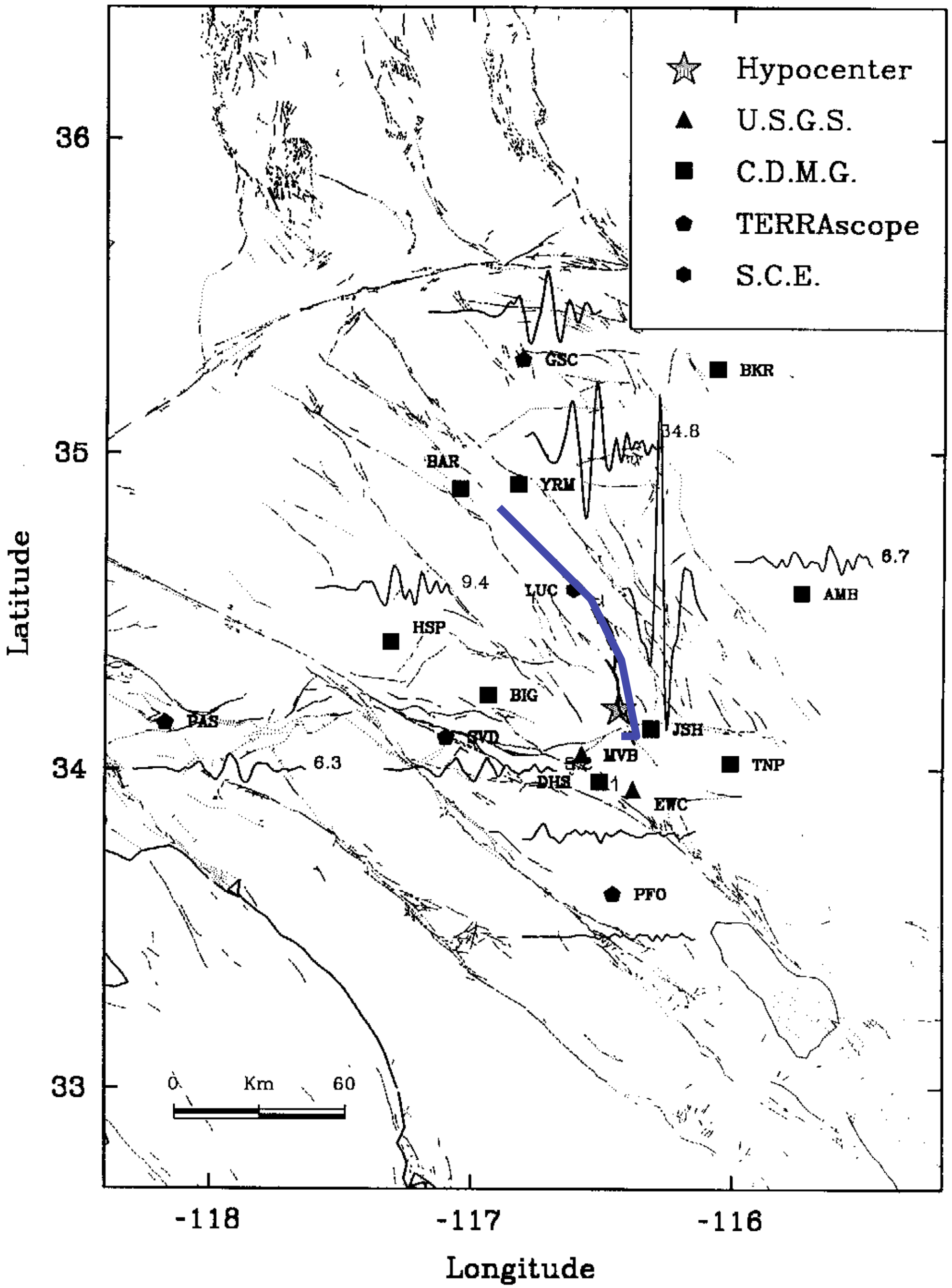

Large variability of ground motion

GPS

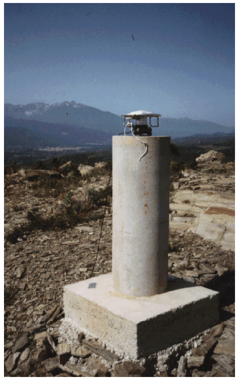

Constellation of satellites
altitude : 20200 km

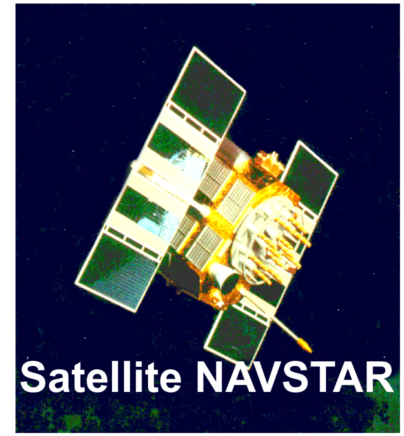

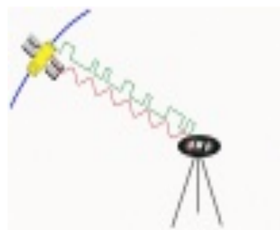

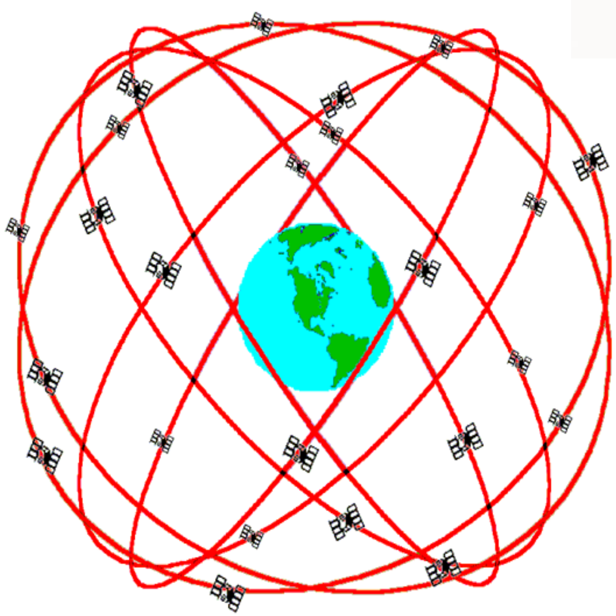

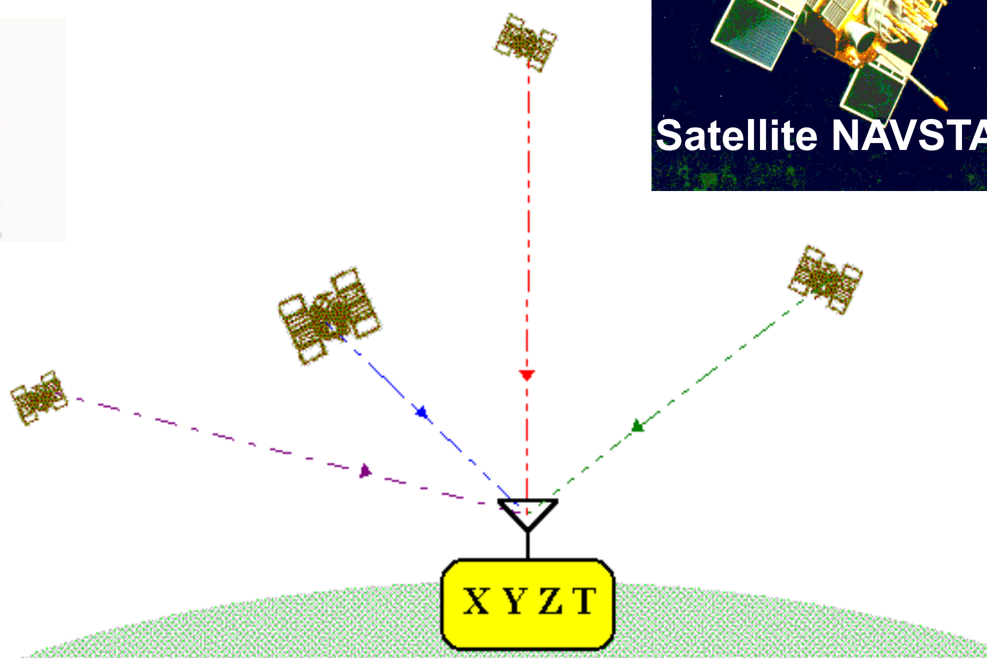

Antennaes :
Precision < 1 cm

RADAR Interferometry

$$\Delta\varphi = \frac{4\pi\Delta d}{\lambda}[2\pi]$$

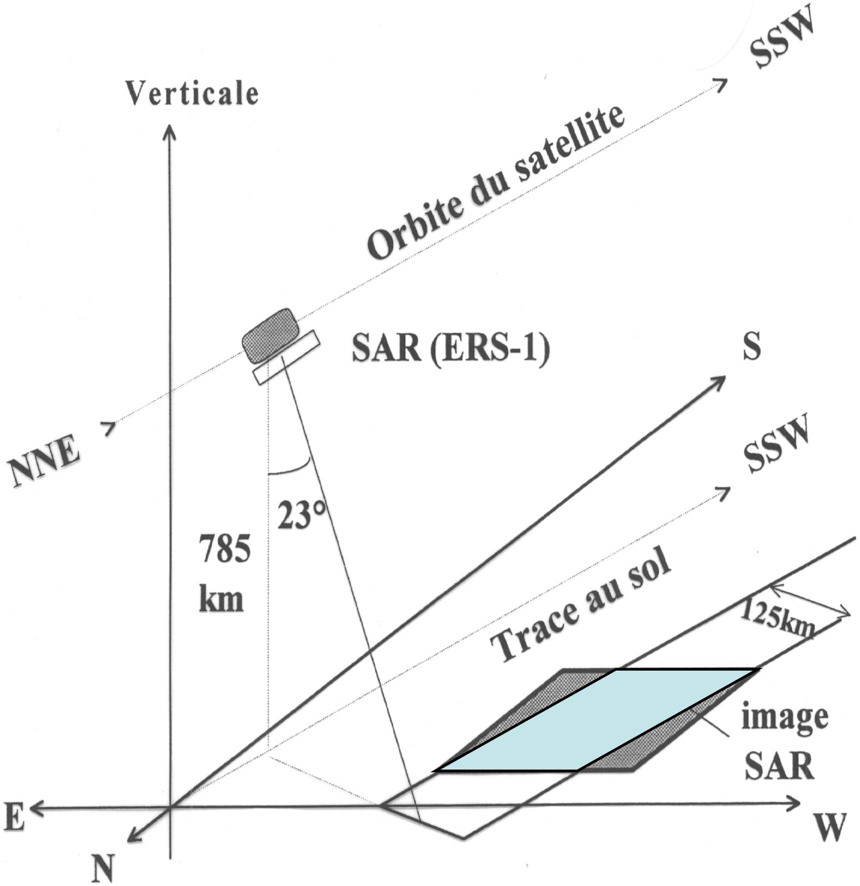

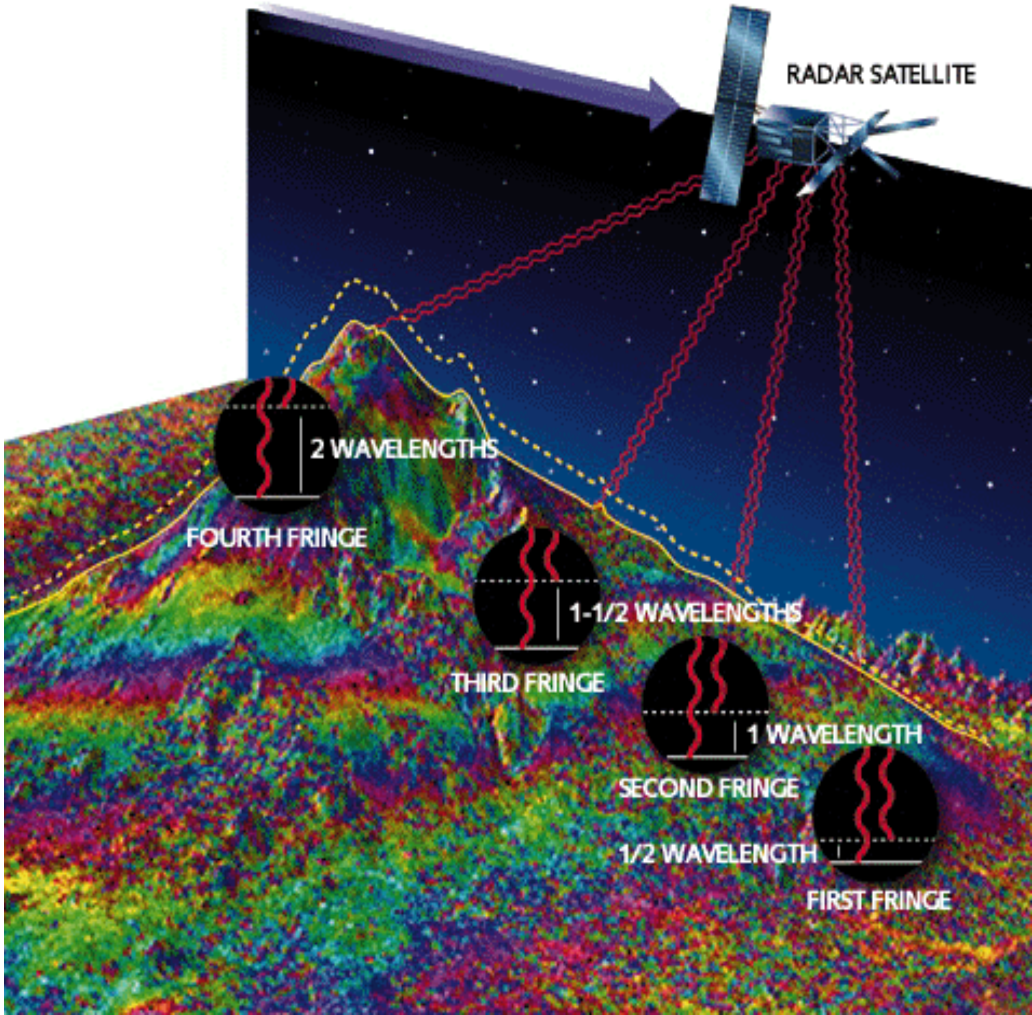

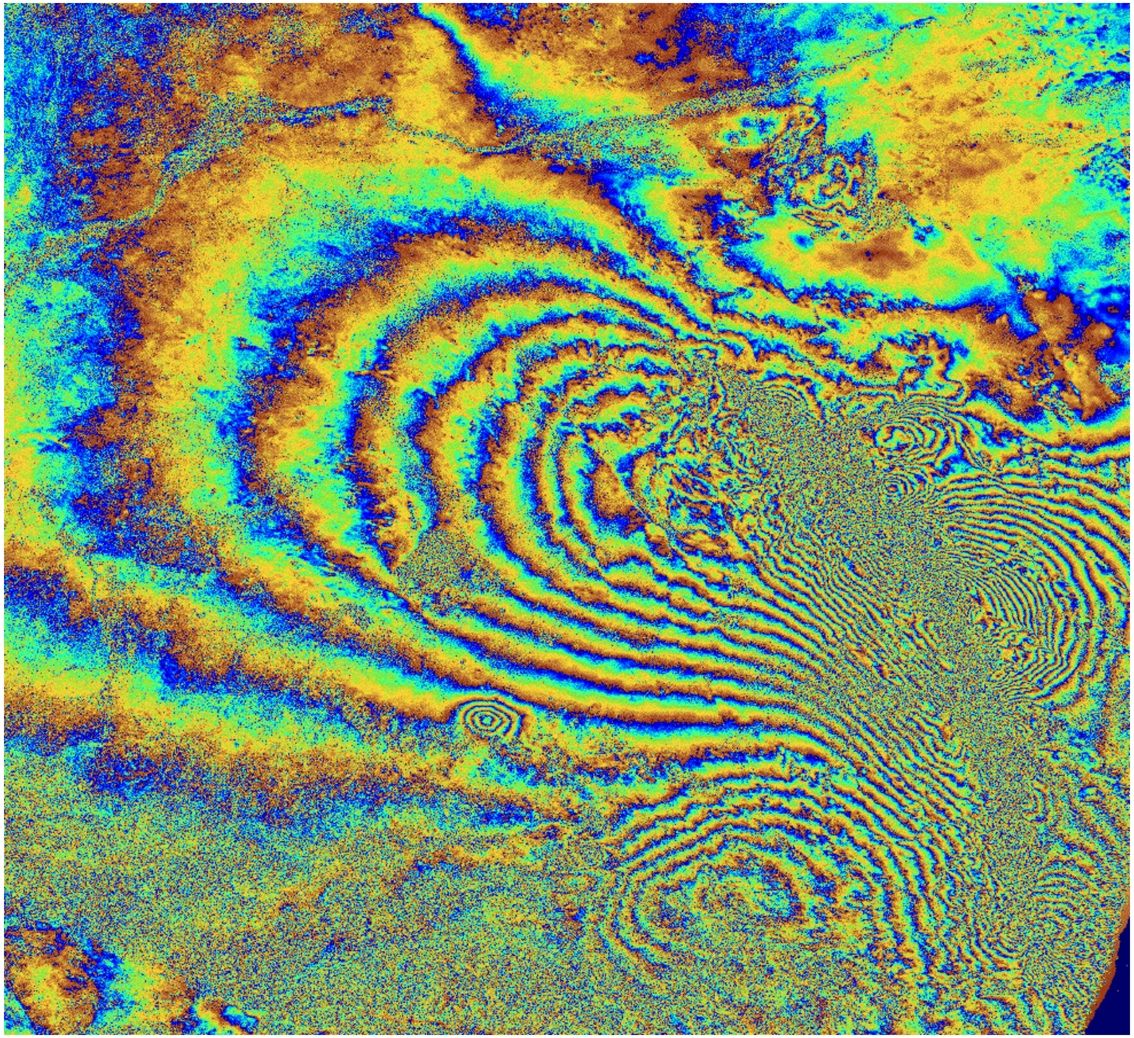

120km x 120 km

Massonnet et al., 1993

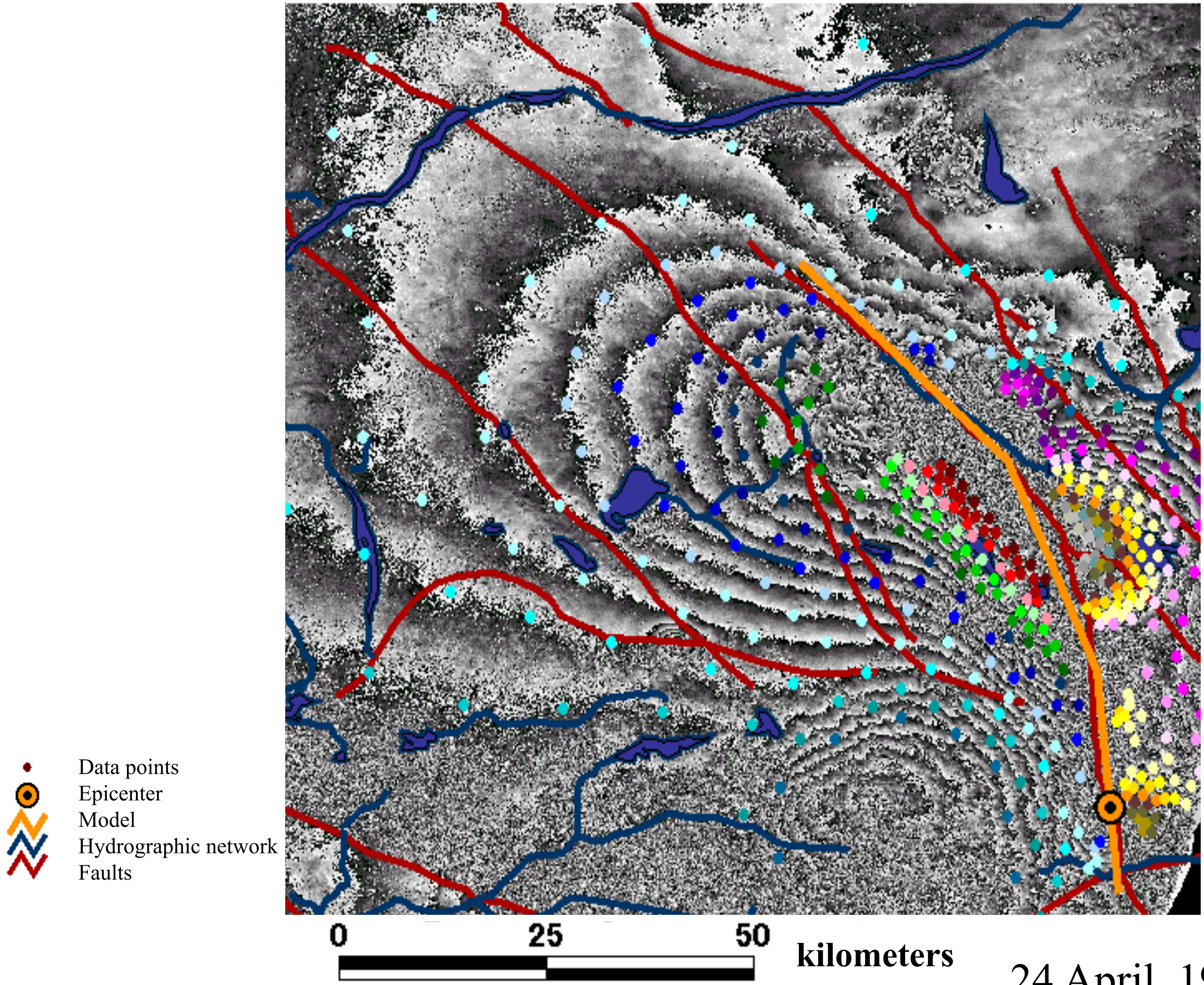

Massonnet et al., 1994

24 April, 1992 - 18 June, 1993

Representation of the fault

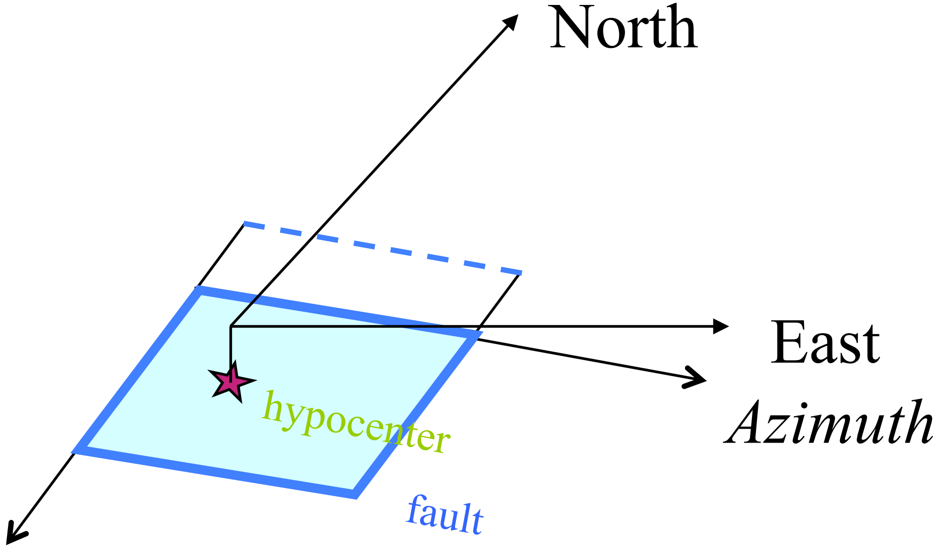

➔ sub-fault

Point sources

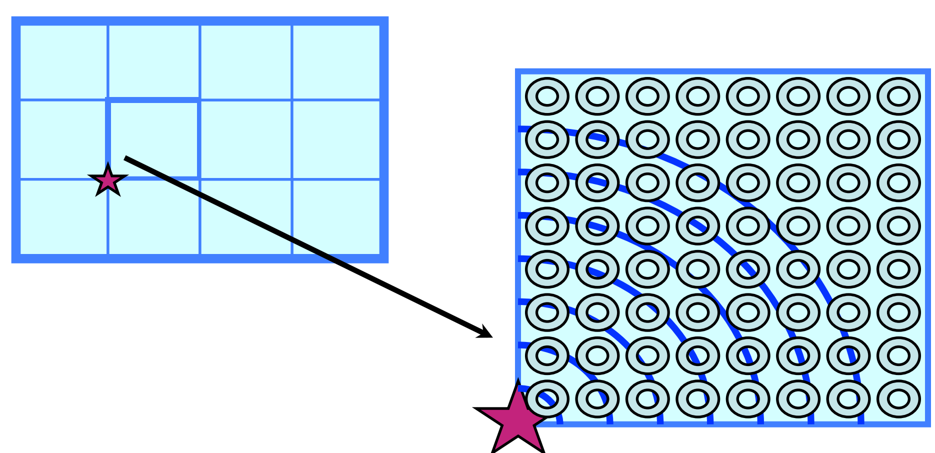

Hypocenter

Aftershock distribution

Moment, focal mechanism

Slip on the fault

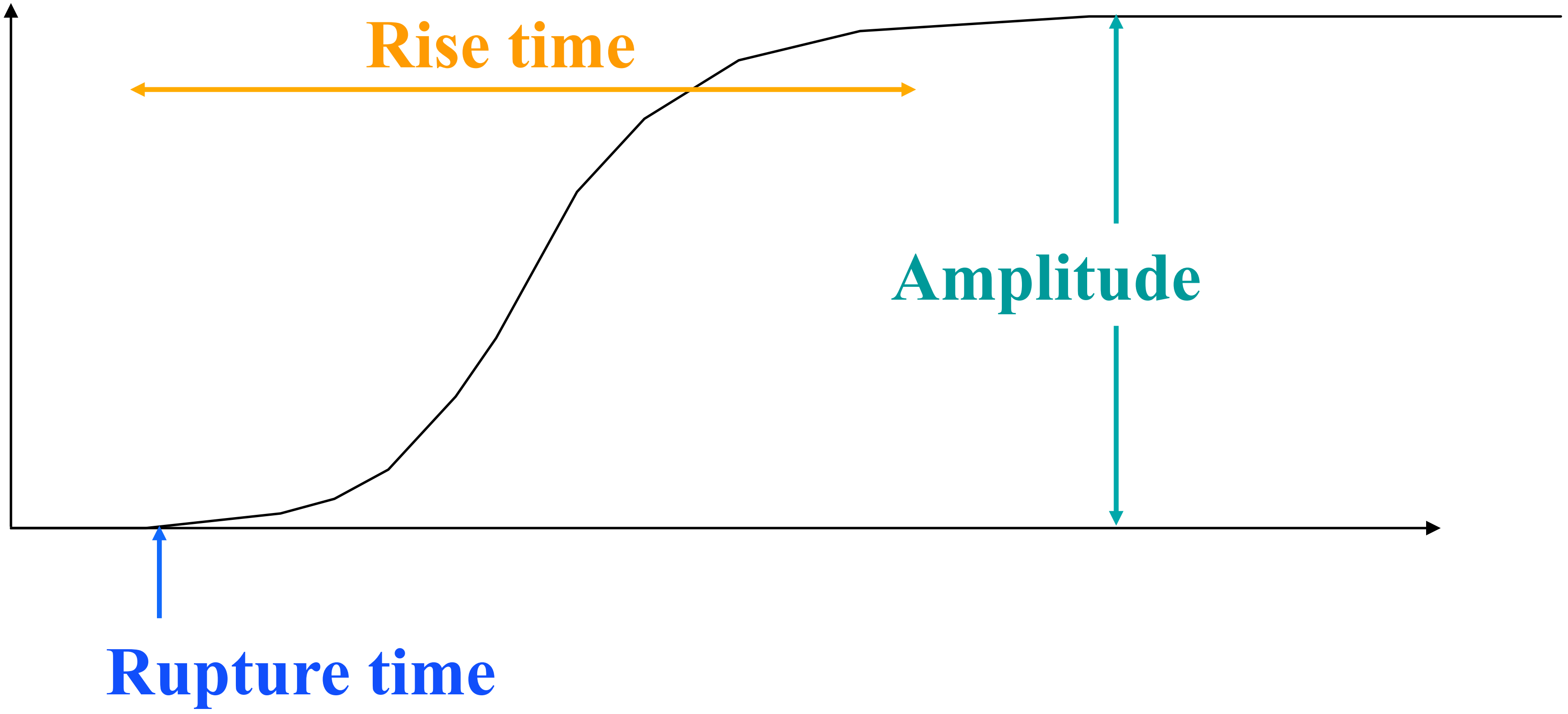

Direct formulation

For station *i* at frequency *ω*

$$u_i(\omega) = \sum_{k=1}^{N} (A_k)\, S(\tau_k, \omega) exp(-i\omega t_k) G_{k,i}(\omega))$$

Sum over the subfaults *k*

amplitude

Rise time

Rupture time

Displacement produced by 'unitary' subfault *k*

Earth model

Elastic response to a dislocation

depth, km	Vp km s^{-1}	Vs km s^{-1}	Density kg cm^{-3}	Qp	Qs
0–2	4,1	2,3	2,5	300	300
2–4	5,5	3,2	2,8	500	500
4–26	6,3	3,65	2,9	500	500
26–32	6,8	3,9	3,1	500	500
32–	8,2	4,7	3,2	500	500

Simulation

synthetics [0 ; 1,5] Hz

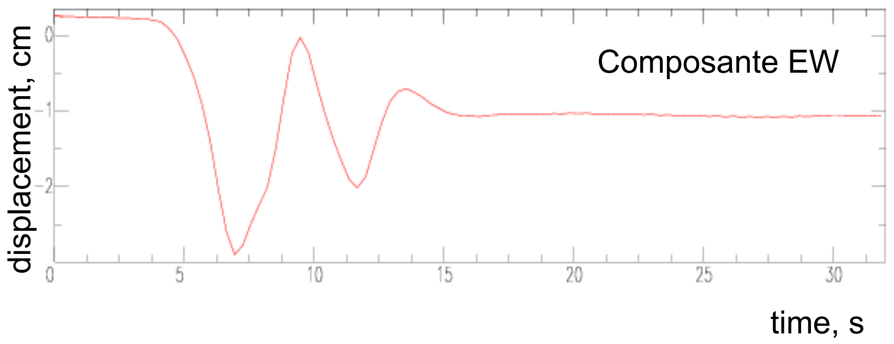

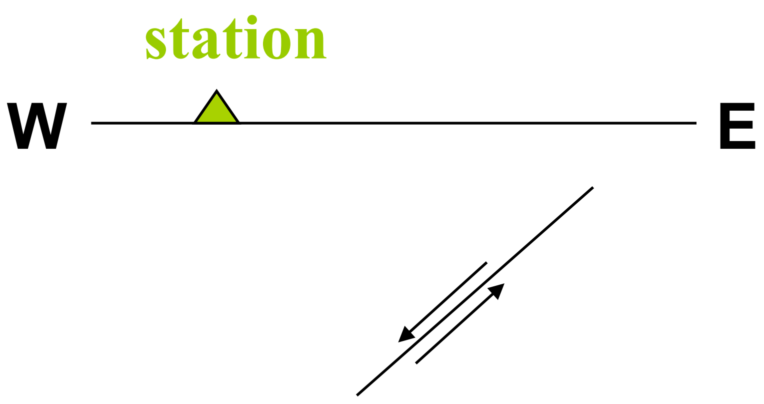

Seismic data ([0,1 ; 1,5] Hz) and geodetic data (f # 0 Hz)

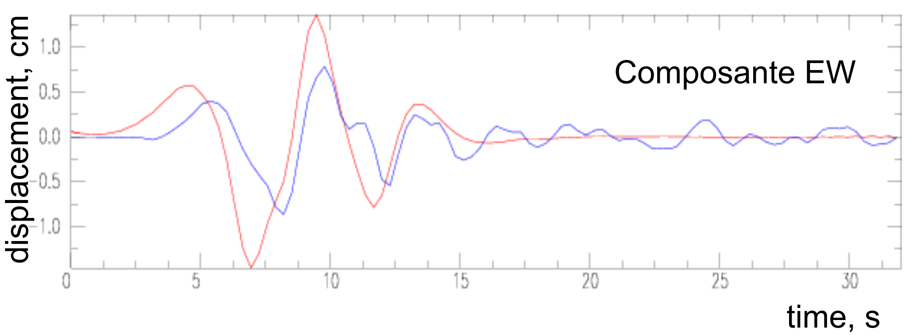

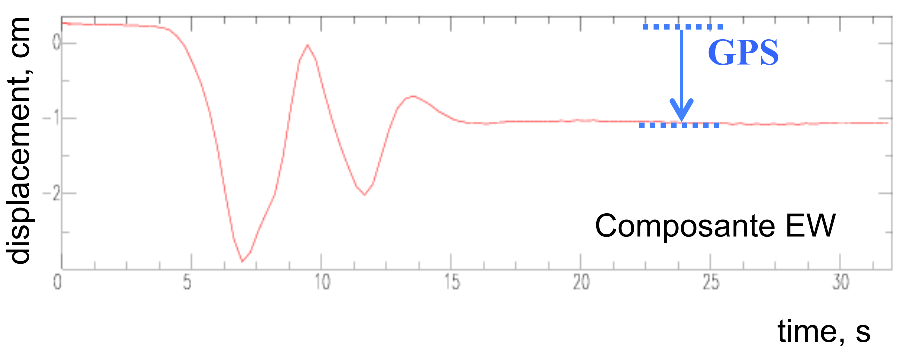

Inversion linéaire : diverses problèmes d'imagerie

Direct problem (simulation)

s = G.m

m: starting model

s: observables

Inverse problem:

s is given

Find m

Optimization

Example of solutions: damped least squares

$$m' = m_0 + (G^t C_d^{-1} G + C_{m_0}^{-1})^{-1} G^t C_d^{-1} (d - G_{m_0})$$

a priori smoothing if the solution

$$C_{m_0}(i,j) = \sigma_i \sigma_j e^{-\left(\frac{d^2(i,j)}{2l^2}\right)}$$

Resolution: measure of the quality

$$R = (G^t C_d^{-1} G + C_{m_0}^{-1})^{-1} G^t C_d^{-1} G$$

+ genetic algorithm, Monte-Carlo, simulated annealing…..

Inversion example: genetic algorithm

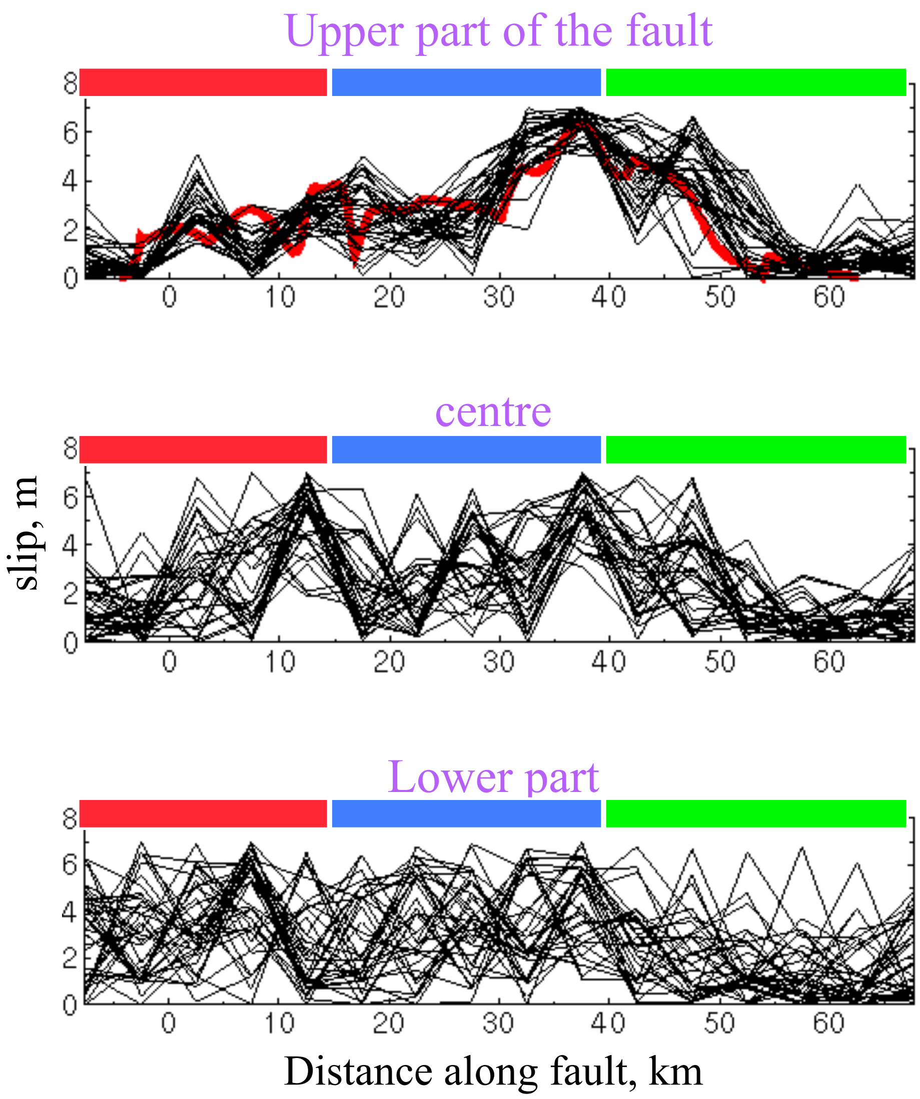

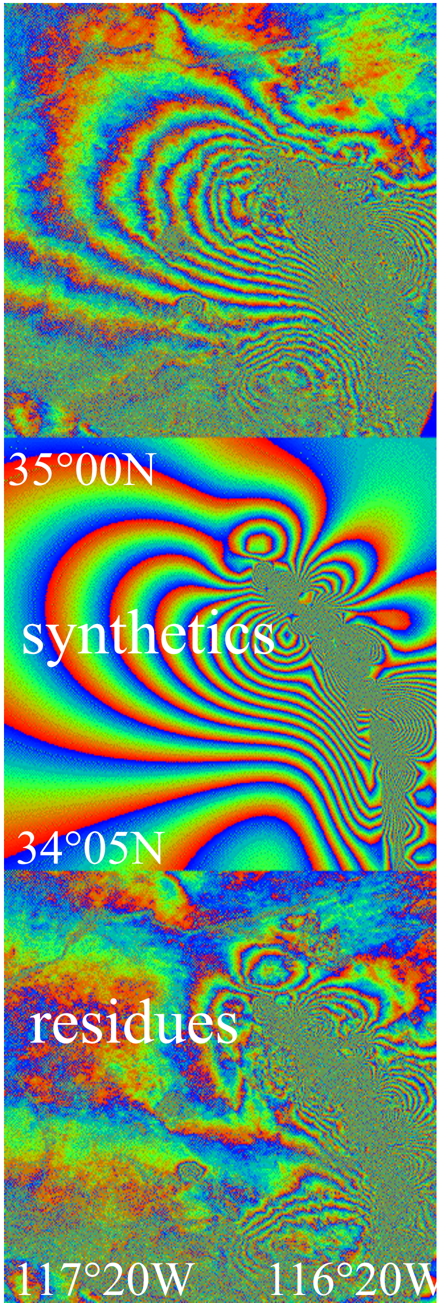

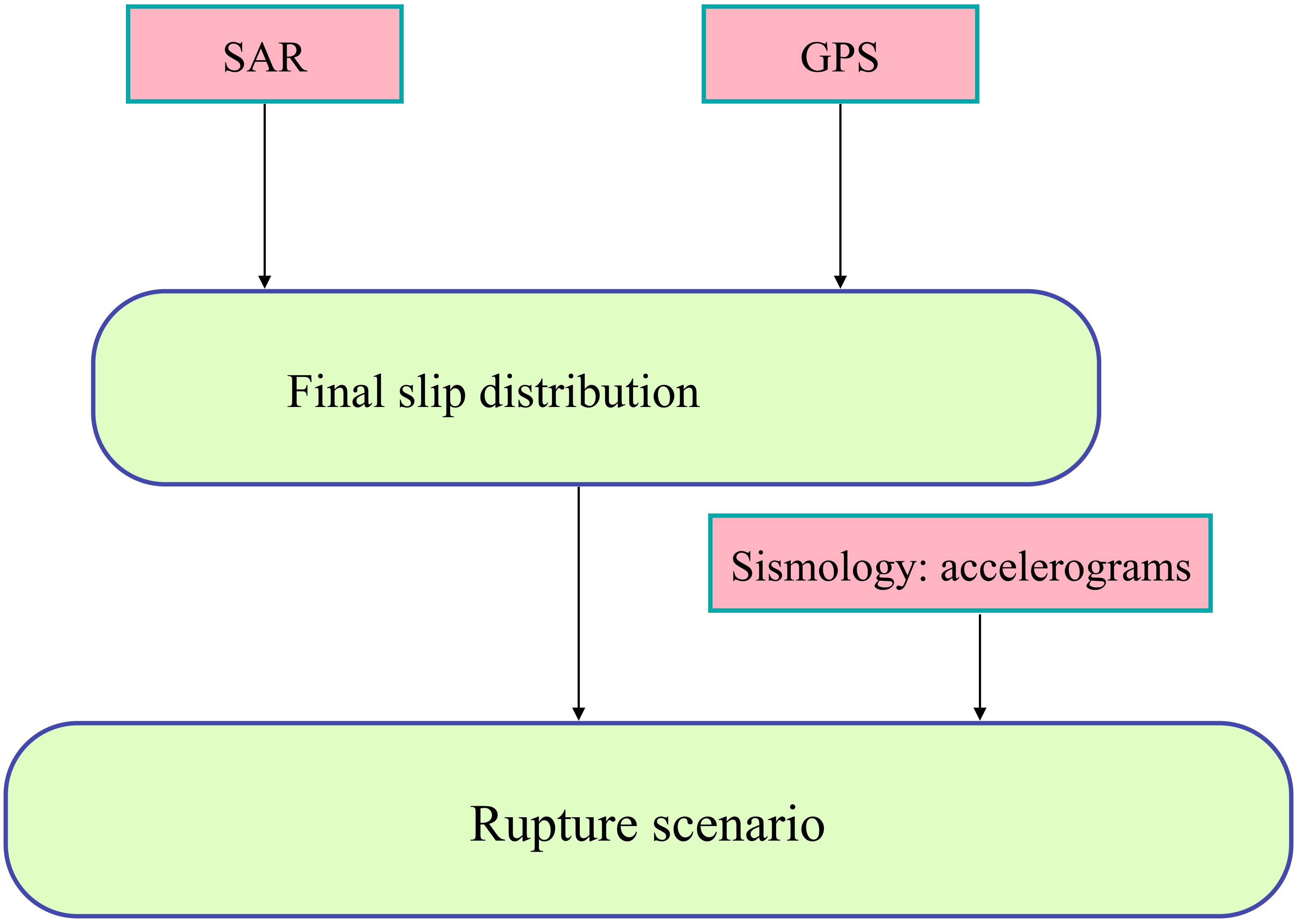
SAR
GPS
Final slip distribution
Sismology: accelerograms
Rupture scenario

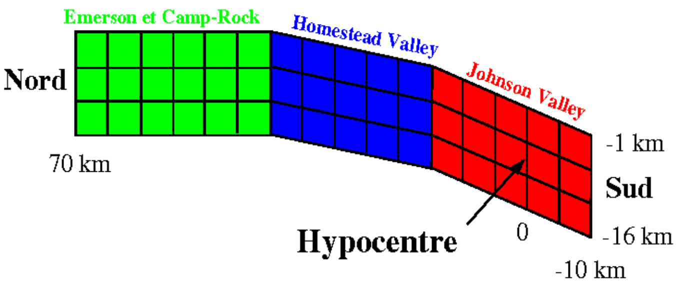

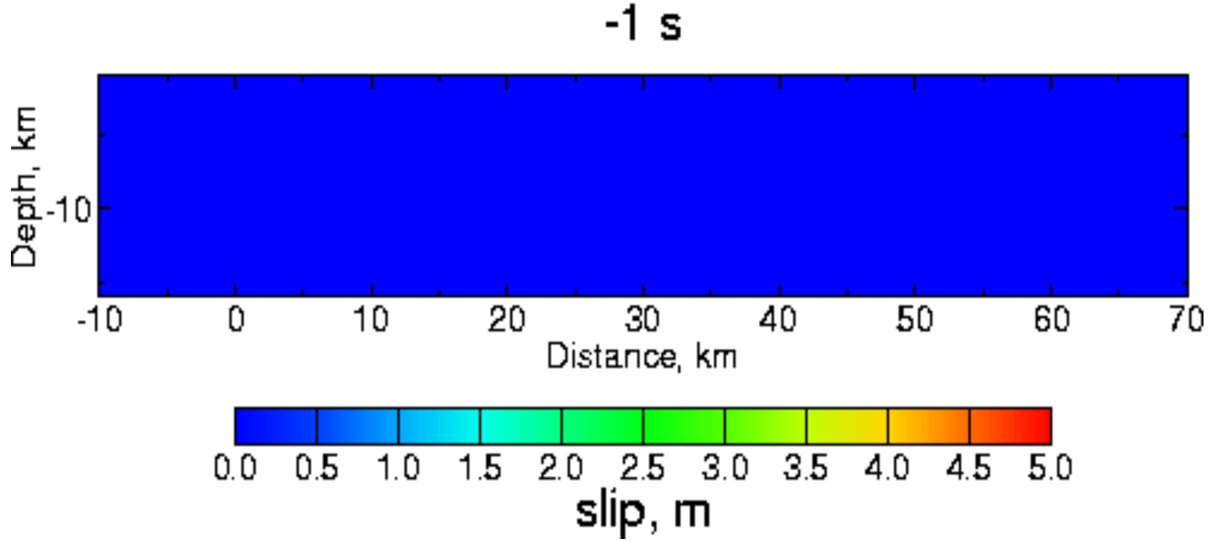

Hernandez et al., 2000

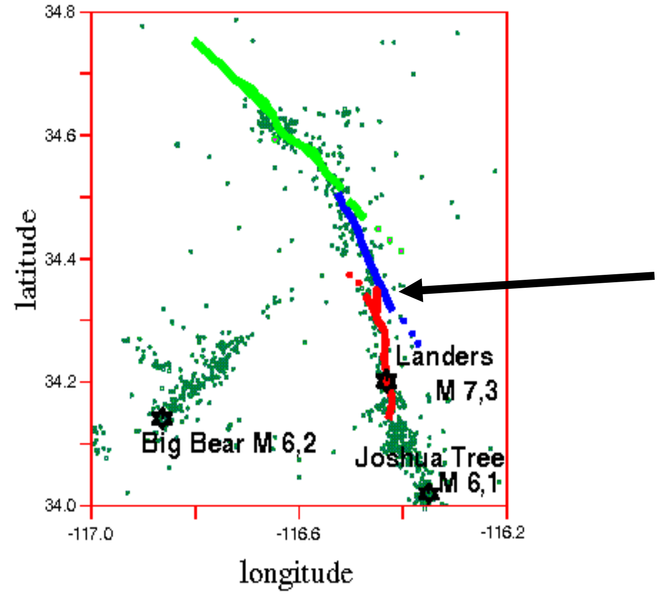

34.8
34.6
34.4
34.2
34.0
latitude
-117.0
-116.6
-116.2
longitude
Landers
M 7,3
Big Bear M 6,2
Joshua Tree
M 6,1

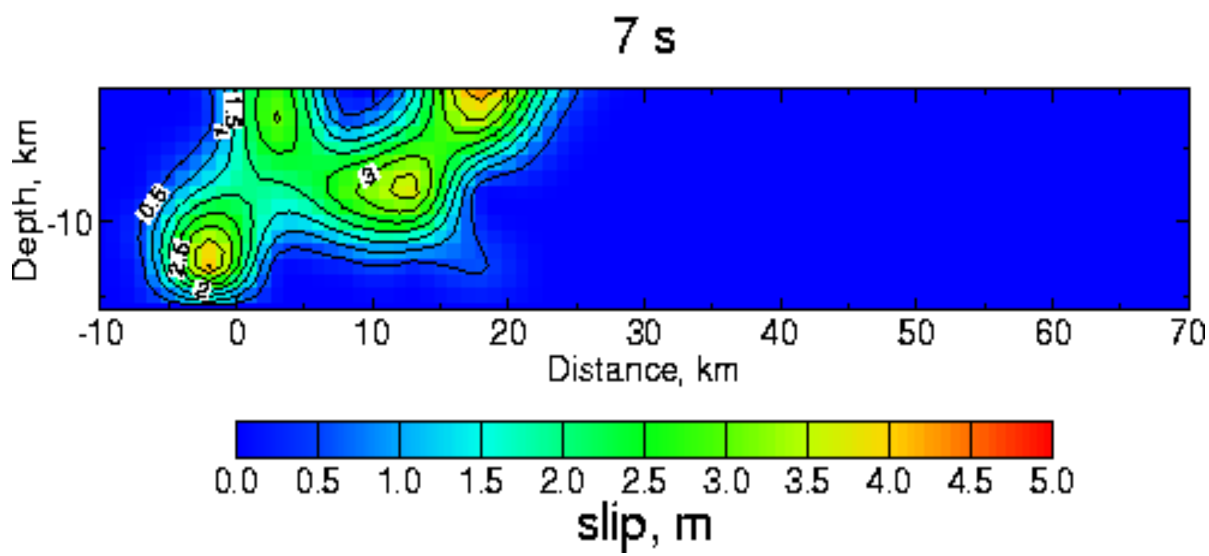

7 s
Depth, km
-10
-10
0
10
20
30
40
50
60
70
Distance, km
0.0
0.5
1.0
1.5
2.0
2.5
3.0
3.5
4.0
4.5
5.0
slip, m

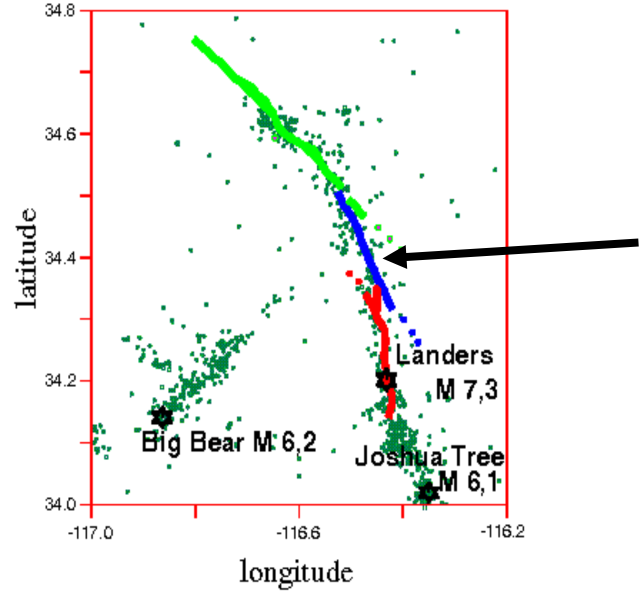
34.8
34.6
34.4
34.2
34.0
latitude
-117.0
-116.6
-116.2
longitude
Landers
M 7,3
Big Bear M 6,2
Joshua Tree
M 6,1

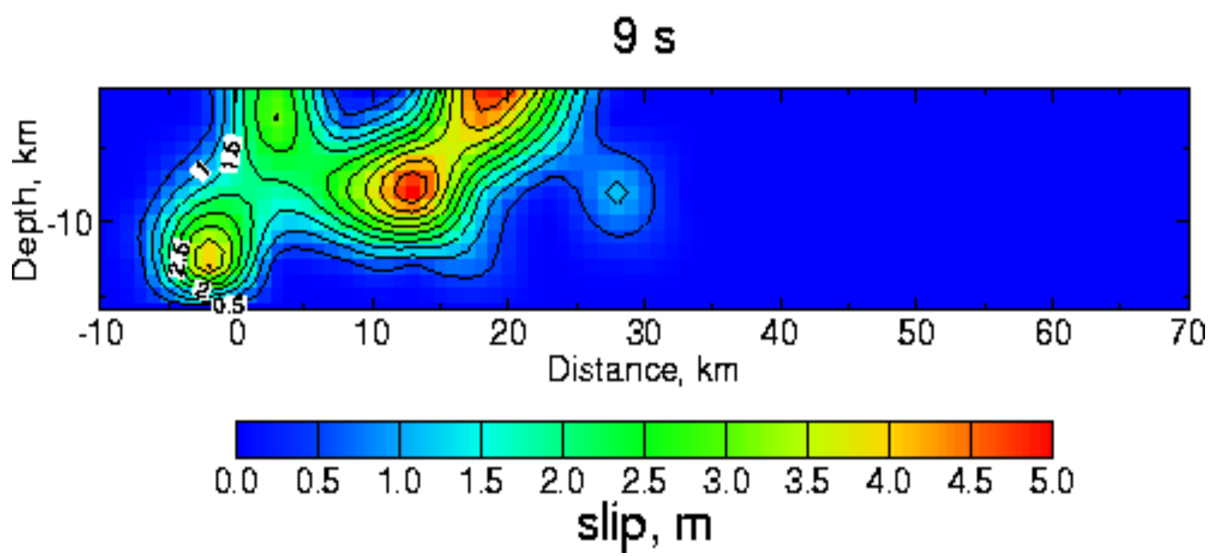
9 s
Depth, km
-10
-10 0 10 20 30 40 50 60 70
Distance, km
0.0 0.5 1.0 1.5 2.0 2.5 3.0 3.5 4.0 4.5 5.0
slip, m

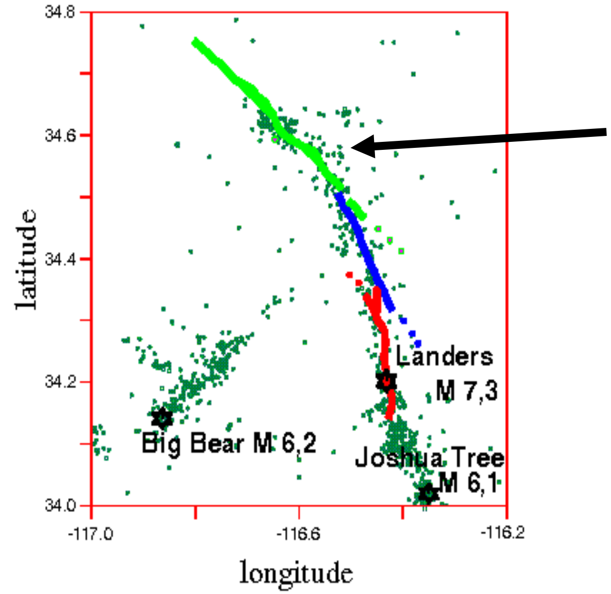
34.8
34.6
34.4
34.2
34.0
latitude
-117.0
-116.6
-116.2
longitude
Landers
M 7,3
Big Bear M 6,2
Joshua Tree
M 6,1

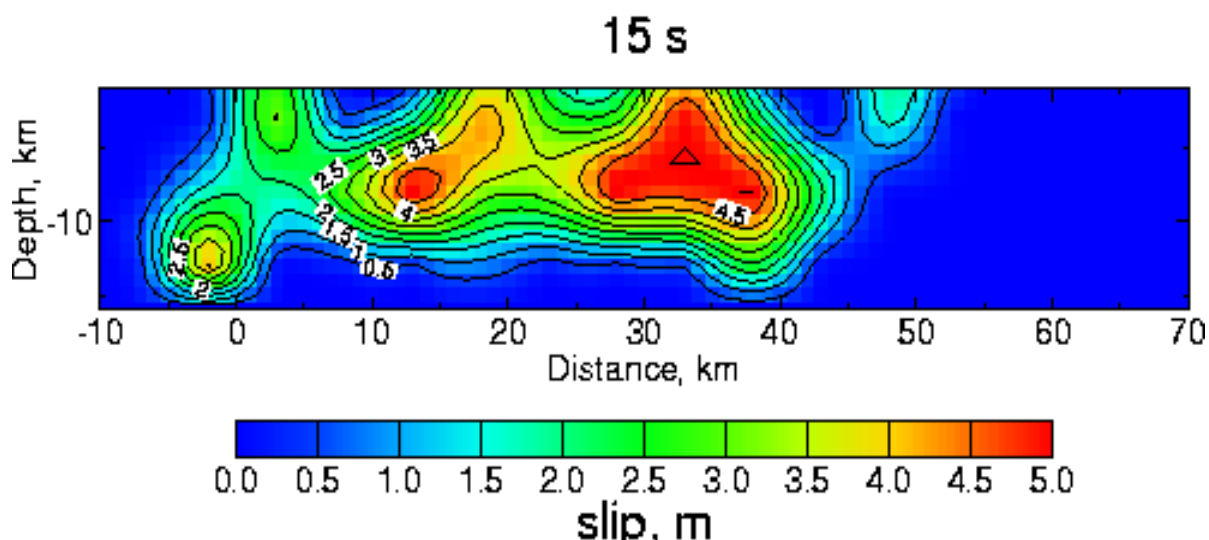
15 s
Depth, km
-10
-10
0
10
20
30
40
50
60
70
Distance, km
0.0
0.5
1.0
1.5
2.0
2.5
3.0
3.5
4.0
4.5
5.0
slip, m

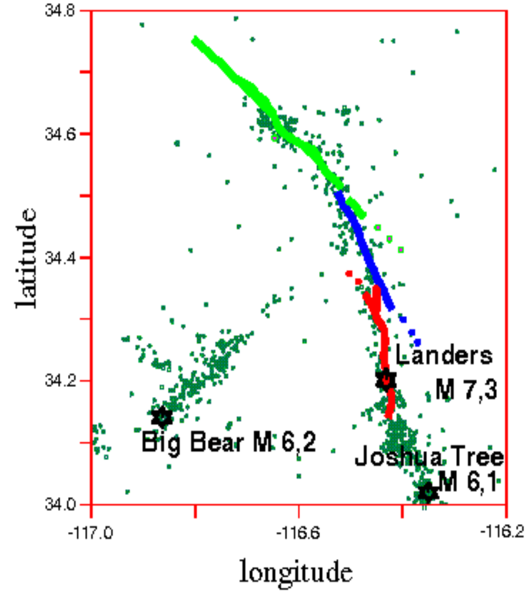
34.8
34.6
34.4
34.2
34.0
latitude
-117.0
-116.6
-116.2
longitude
Landers
M 7,3
Big Bear M 6,2
Joshua Tree
M 6,1

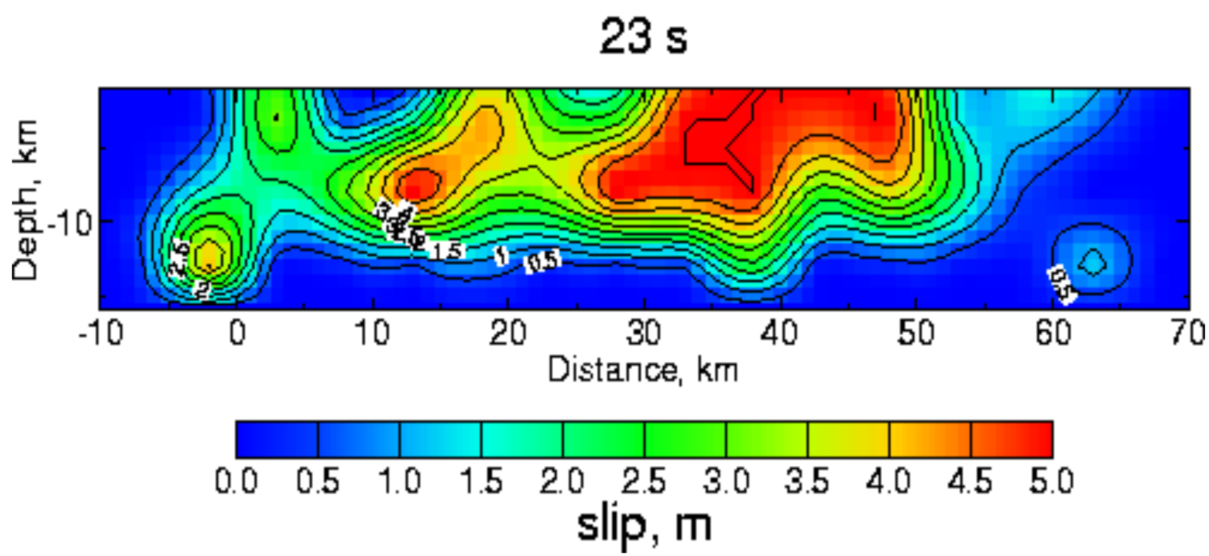
23 s
Depth, km
-10
-10
0
10
20
30
40
50
60
70
Distance, km
0.0
0.5
1.0
1.5
2.0
2.5
3.0
3.5
4.0
4.5
5.0
slip, m

Rupture speed at the surface

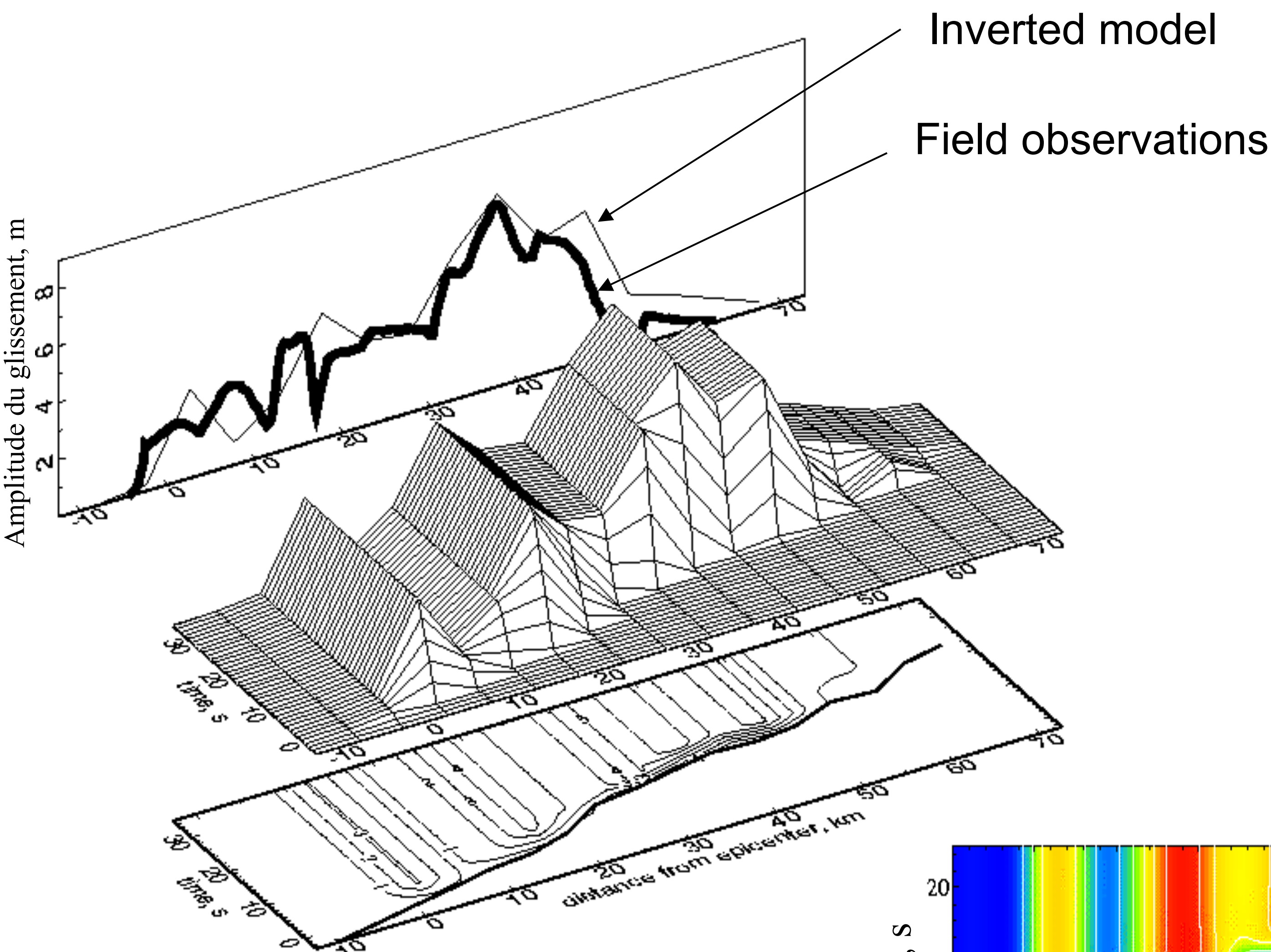

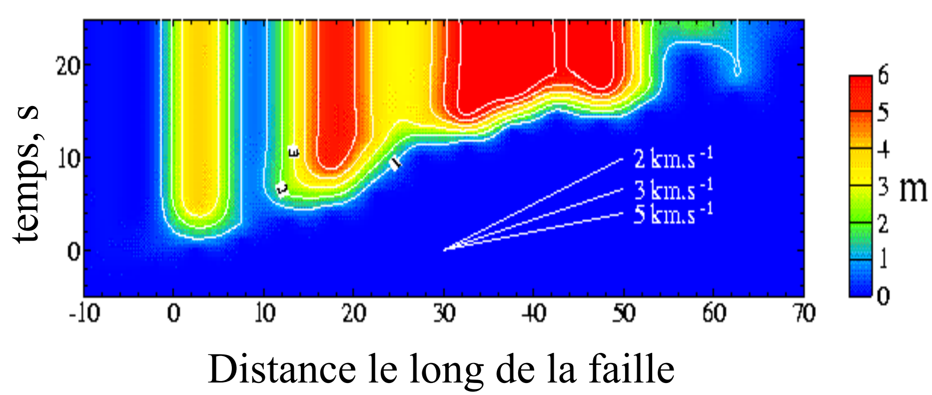

Moment magnitude M_w

Magnitudes saturate:

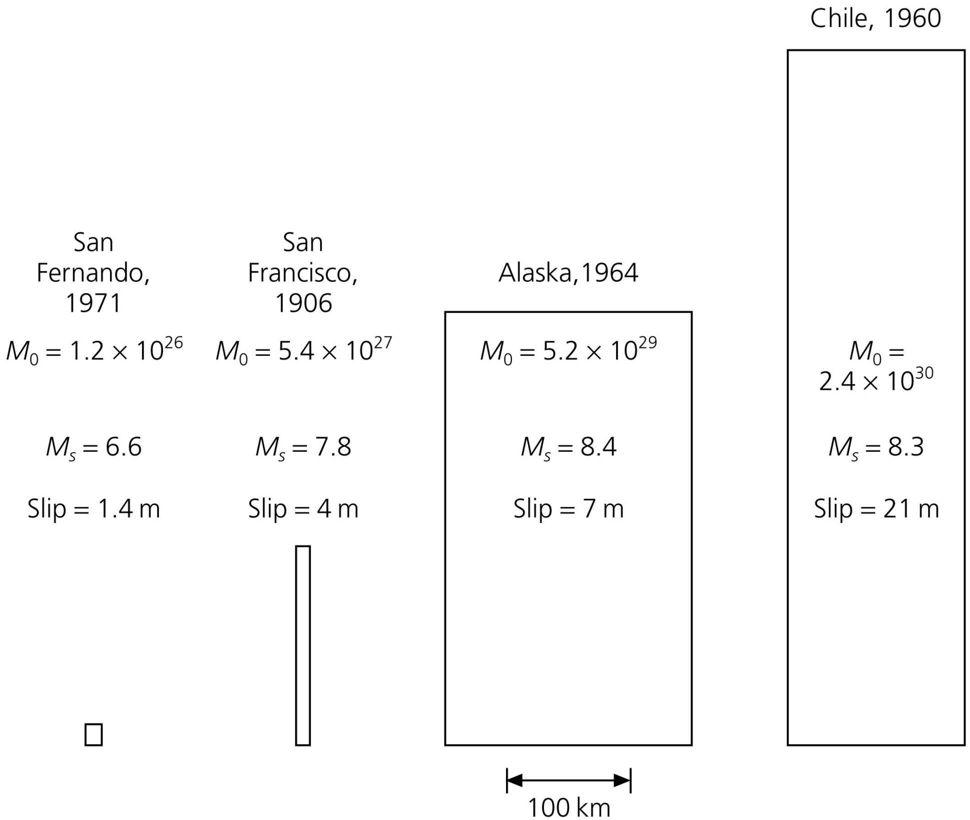

Moment magnitude:

$$M_w = \frac{\log M_0}{1.5} - 10.73$$

(with M_0 in dyn-cm)

Earthquake	Body wave magnitude m_b	Surface wave magnitude M_s	Fault area (km^2) length × width	Average dislocation (m)	Moment (dyn-cm) M_0	Moment magnitude M_w
Truckee, 1966	5.4	5.9	10 × 10	0.3	8.3×10^{24}	5.8
San Fernando, 1971	6.2	6.6	20 × 14	1.4	1.2×10^{26}	6.7
Loma Prieta, 1989	6.2	7.1	40 × 15	1.7	3.0×10^{26}	6.9
San Francisco, 1906		8.2	320 × 15	4	6.0×10^{27}	7.8
Alaska, 1964	6.2	8.4	500 × 300	7	5.2×10^{29}	9.1
Chile, 1960		8.3	800 × 200	21	2.4×10^{30}	9.5

SOURCE PULSE FROM EARTHQUAKE

TIME DURATION =

Figure 4.3-3: Derivation of a trapezoidal source time function.

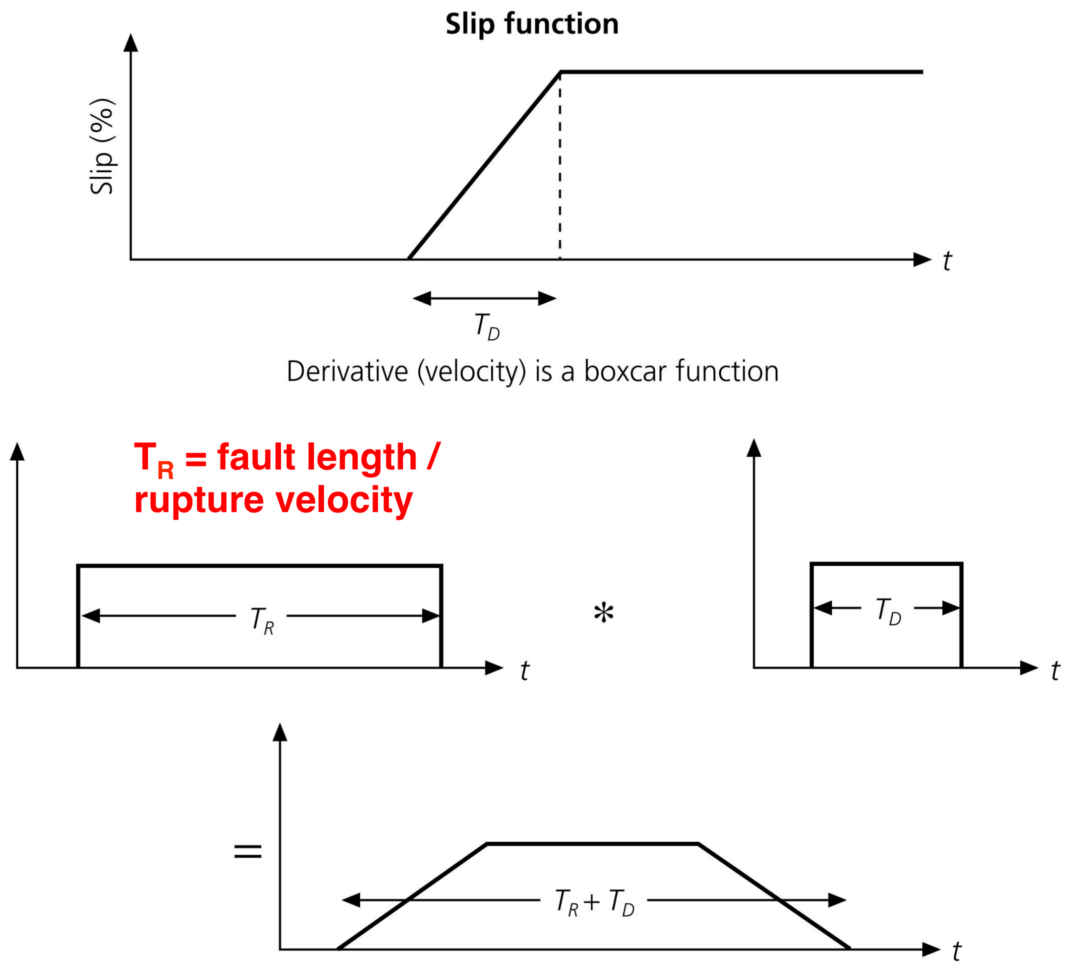

What would this source time function look like in the frequency domain?

SPECTRUM OF SOURCE TIME FUNCTION

The transform of a boxcar of height $1/T$ and length T is

$$F(\omega) = \int_{-T/2}^{T/2} \frac{1}{T} e^{i\omega t} dt = \frac{1}{Ti\omega}\left(e^{i\omega T/2} - e^{-i\omega T/2}\right) = \frac{\sin(\omega T/2)}{\omega T/2}$$

(has the form of a "sinc" function: $\mathrm{sinc}\ x = (\sin x)/x$)

The spectral amplitude of the source signal is the product of the seismic moment and two sinc terms

$$|A(\omega)| = M_0 \left|\frac{\sin(\omega T_R/2)}{\omega T_R/2}\right| \left|\frac{\sin(\omega T_D/2)}{\omega T_D/2}\right|$$

T_R and T_D are the rupture and rise times.

$$\log\ A(\omega) = \log\ M_0 + \log\left[\mathrm{sinc}(\omega T_R/2)\right] + \log\left[\mathrm{sinc}(\omega T_D/2)\right]$$

Approximation of the amplitude spectrum of a trapezoidal box car function:

$$\log|A(\omega)| =$$

$$= \left\{ \begin{array}{cc} \log M_0 & \omega < 2/T_R \\ \log M_0 - \log (T_R/2) - \log \omega & 2/T_R < \omega < 2/T_D \\ \log M_0 - \log (T_R T_D/4) - 2 \log \omega & 2/T_D < \omega \end{array} \right\}$$

The spectrum os often defined in terms of the "corner frequencies"

SOURCE SPECTRUM

seismic moment

Corner frequency shifts to left (lower frequency) for larger earthquakes with longer faults

Figure 4.6-4: Approximation of the (sin *x*)/*x* function, and derivation of corner frequencies.

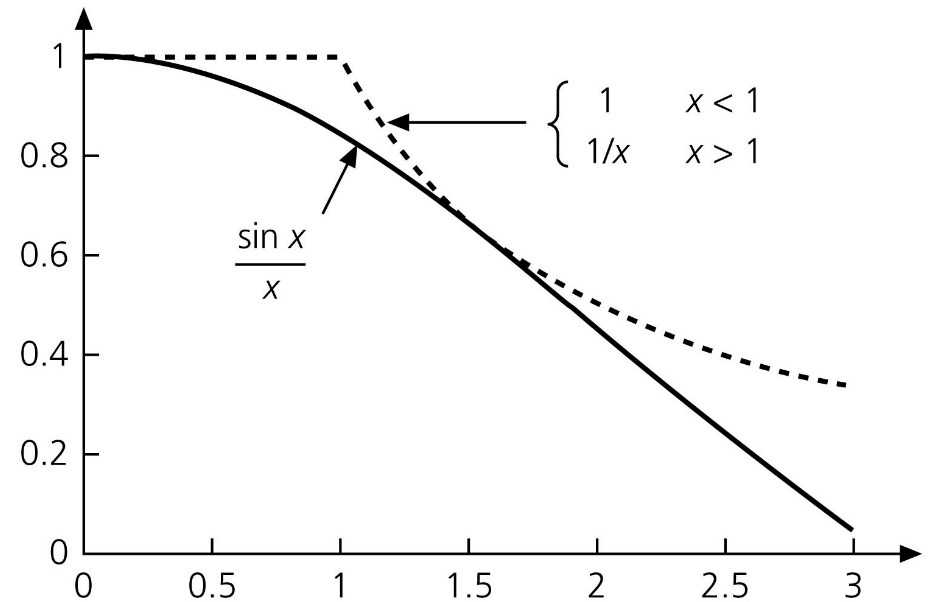

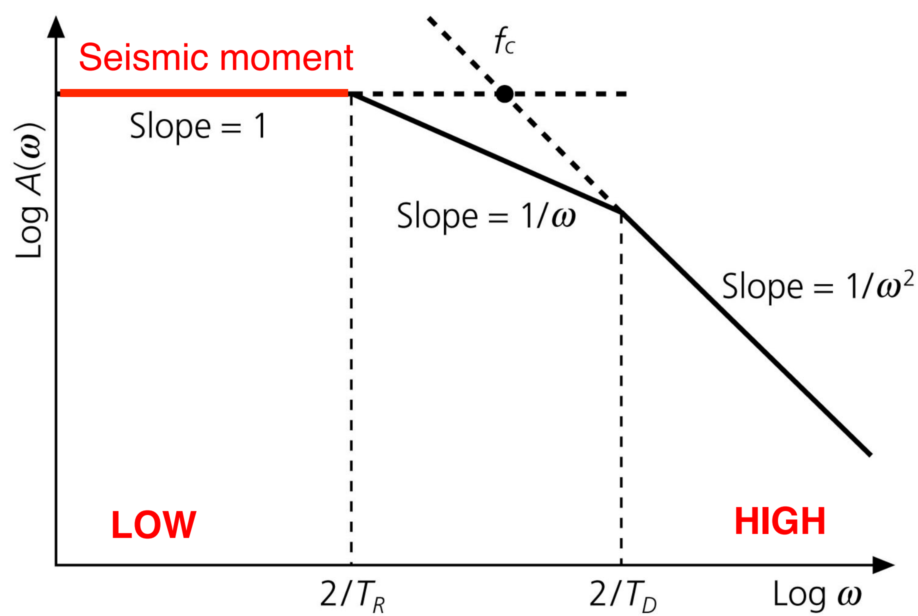

DIFFERENT MAGNITUDES REFLECT ENERGY RELEASE AT DIFFERENT PERIODS

1 s - Body wave magnitude

20 s - Surface wave magnitude

Long period - moment magnitude derived from moment

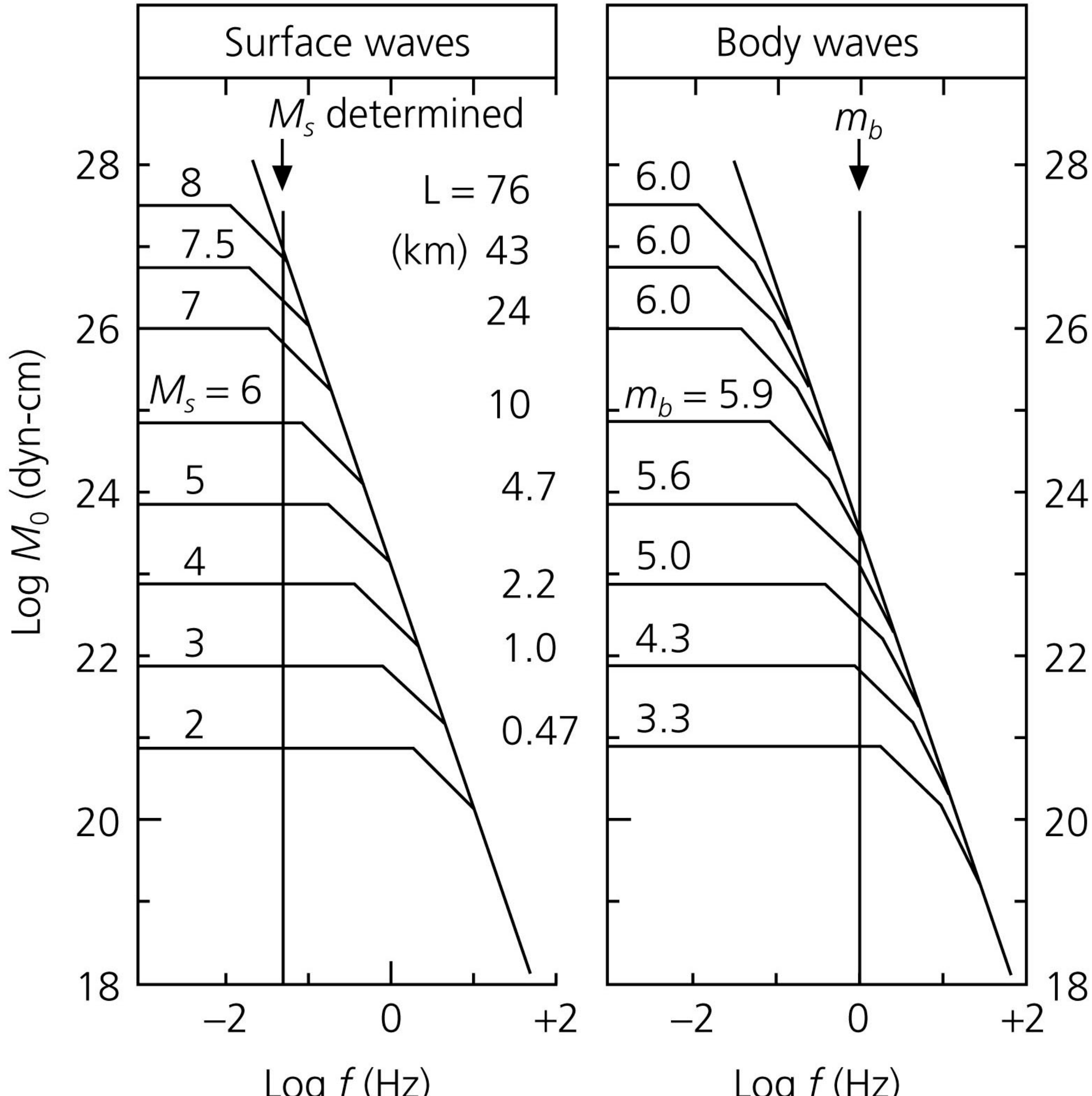

DIFFERENT MAGNITUDE SCALES REFLECT AMPLITUDE AT DIFFERENT PERIODS

Body & surface wave magnitudes

- because added energy release in very large earthquakes is at periods > 20 s

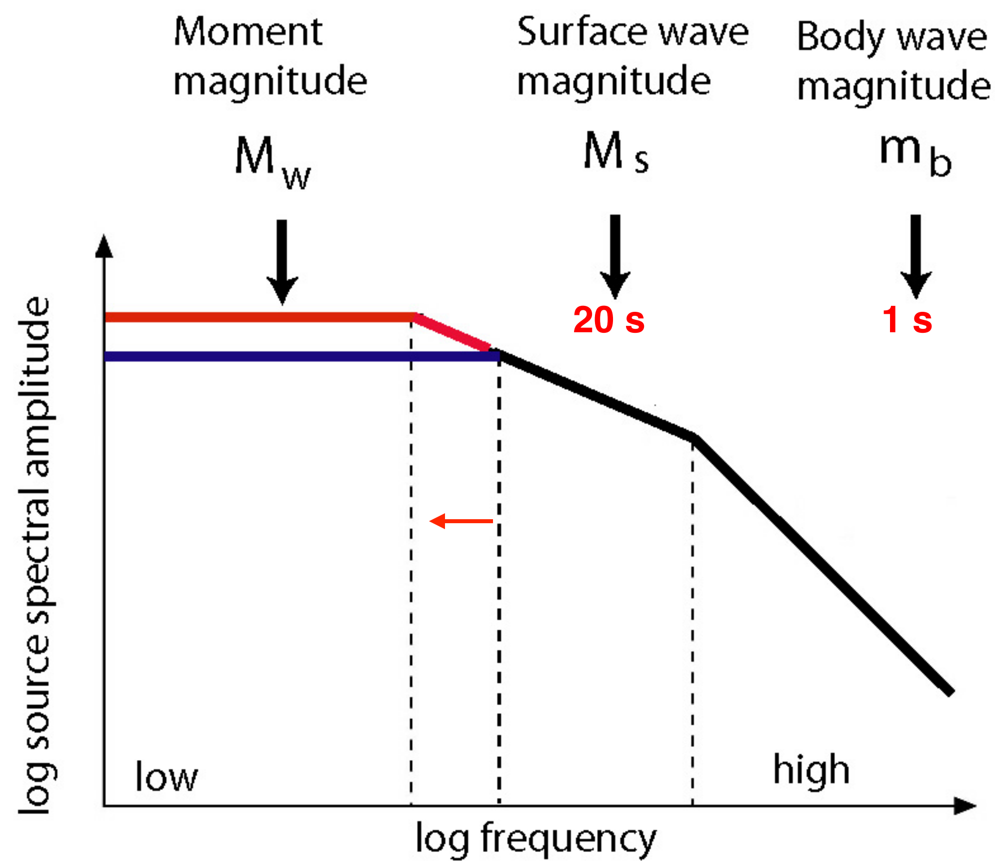

For very large earthquakes only low period moment magnitude reflects earthquake's size.

This issue is crucial for tsunami warning because long periods excite tsunami, but are harder to study in real time

Directivity =

ex: apparent duration-spectrum

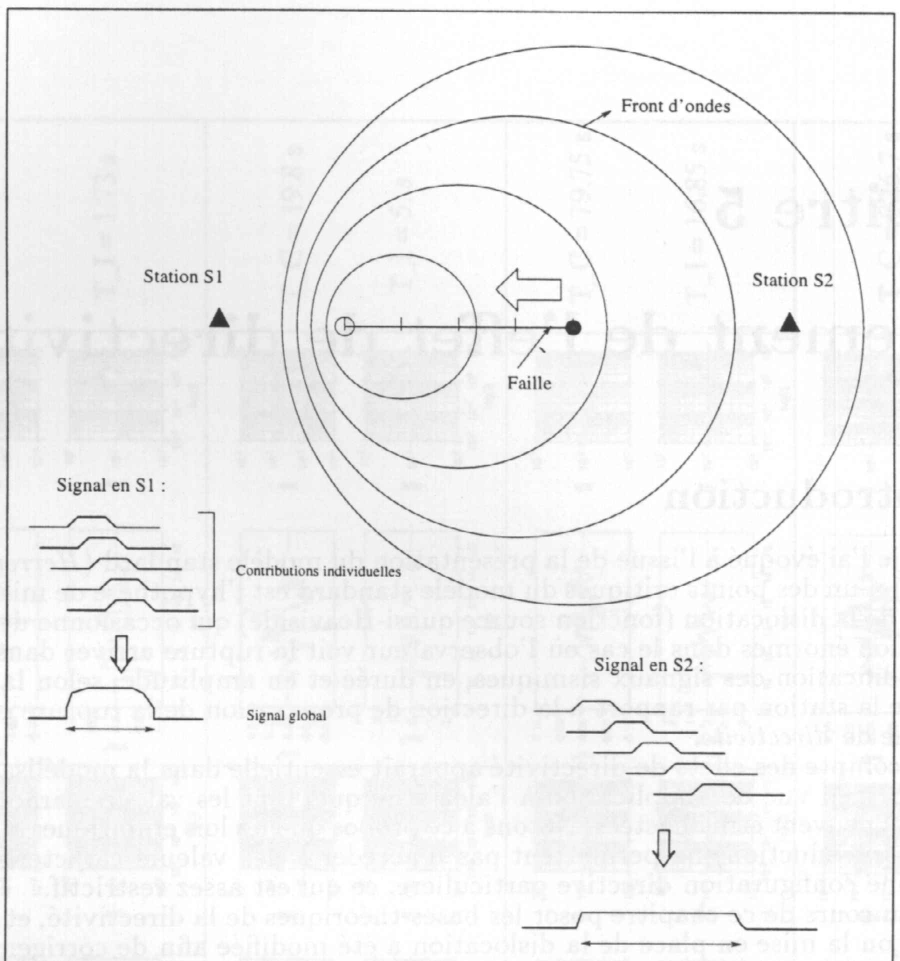

FIG. 5.1 – *Illustration de l'effet de directivité.*

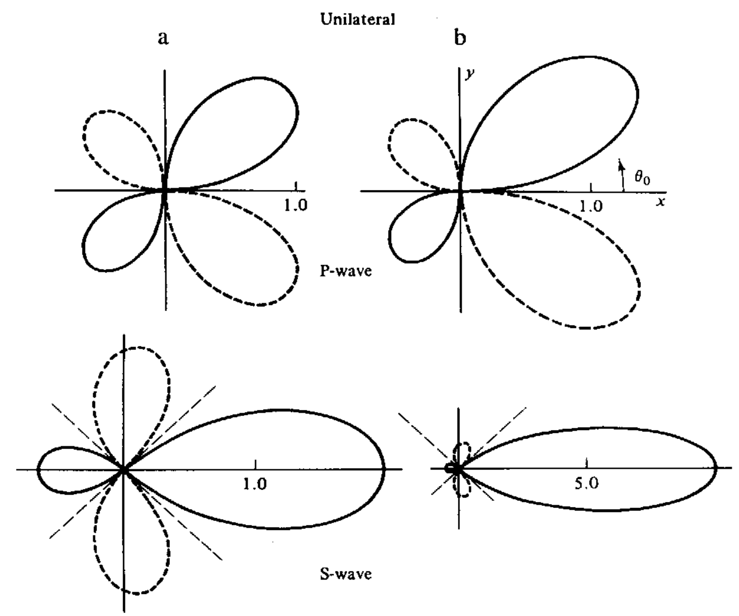

FIGURE 9.10 The variability of *P*- and *SH*-wave amplitude for a propagating fault (from left to right). For the column on the left $v_r/v_s = 0.5$, while for the column on the right $v_r/v_s = 0.9$. Note that the effects are amplified as rupture velocity approaches the propagation velocity. (From Kasahara, 1981.)

Lay et Wallace, 1995, Berge, 1996

Displacement spectrum« ω^{-2} » : spectral decay above f_c

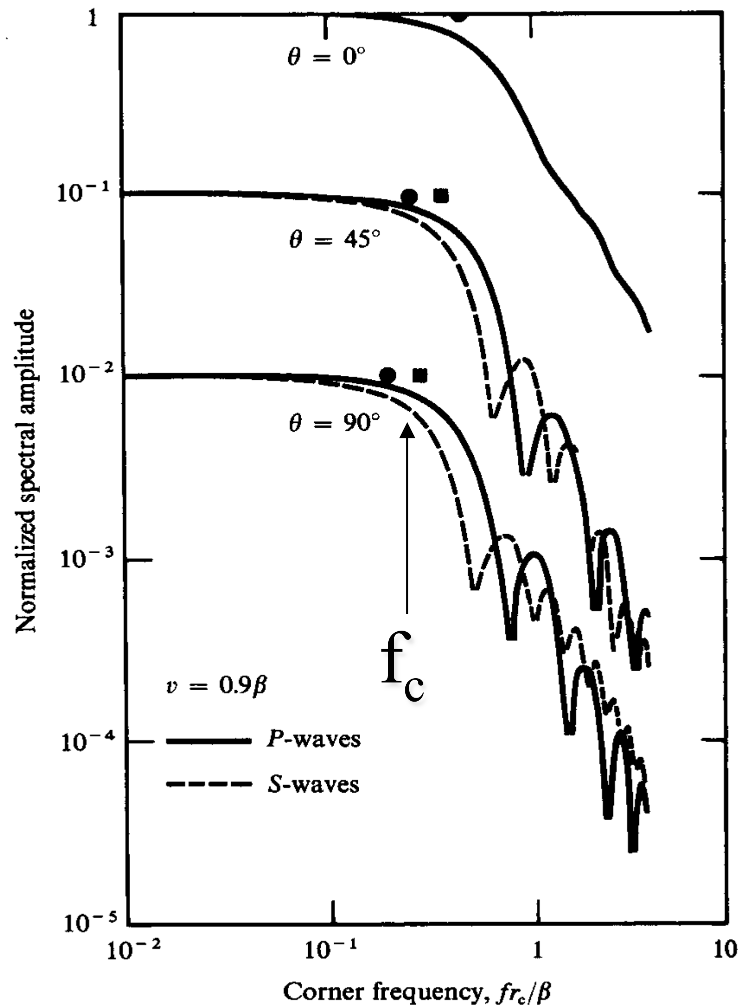

Theory

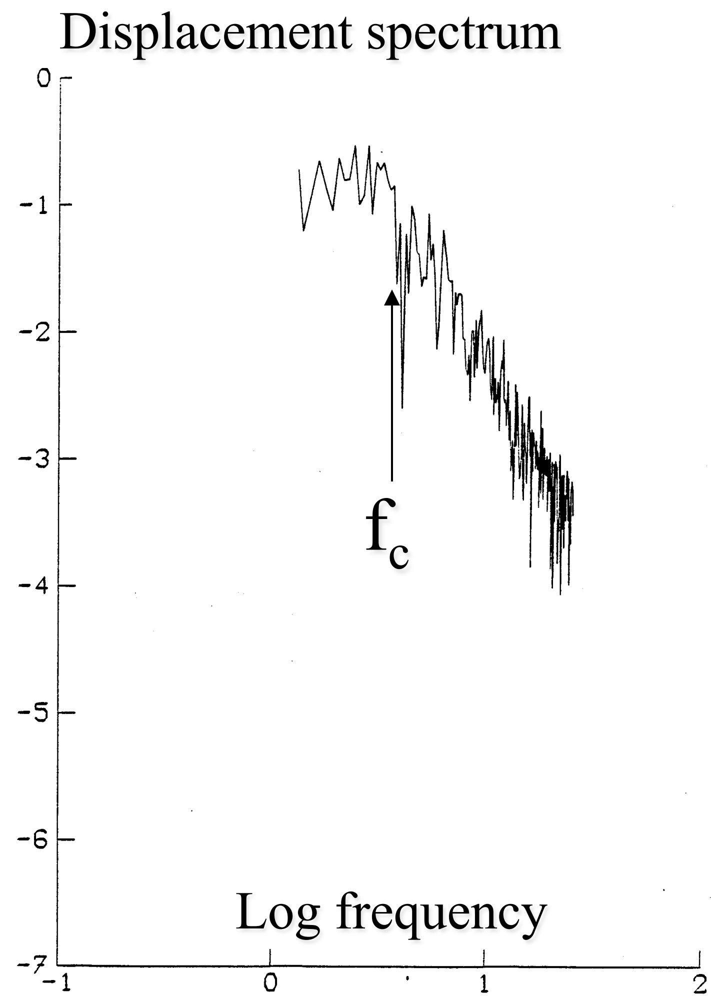

Data

$f_c \sim \beta/a$ ➔ characteristic length ≈ size

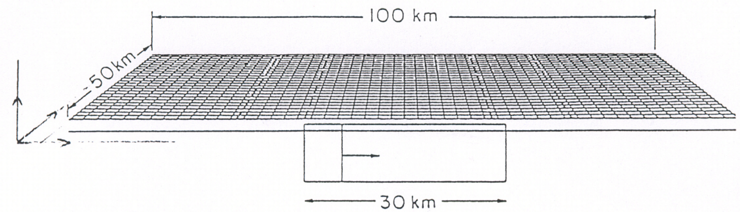
100 km
50 km
30 km

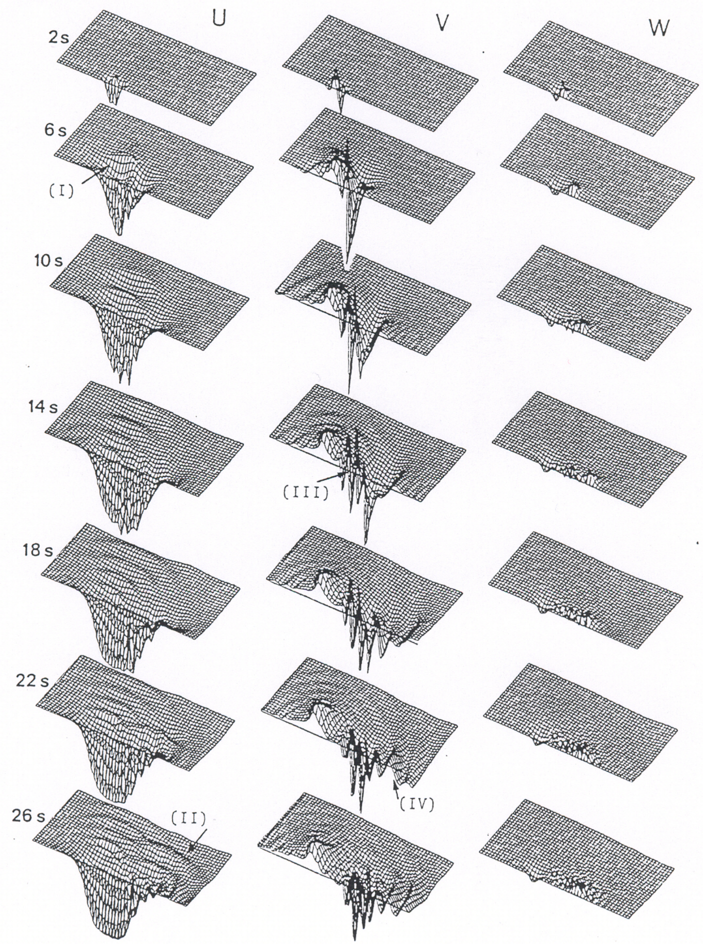
U
V
W
2s
6 s
10 s
14 s
18 s
22 s
26 s
(I)
(II)
(III)
(IV)

Directivity during the Landers earthquake

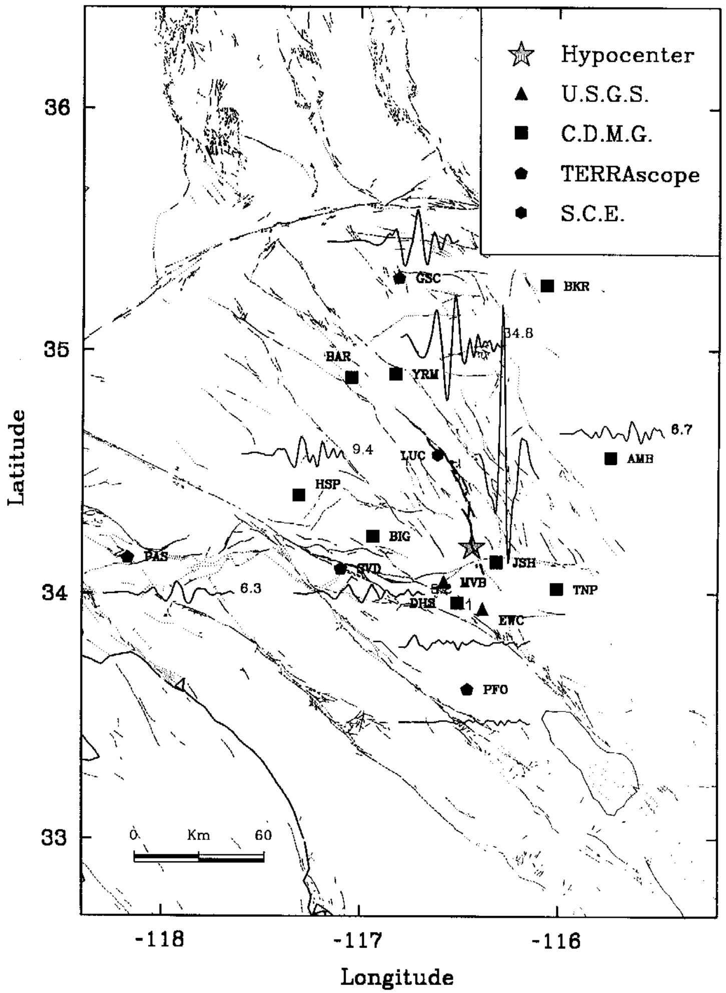

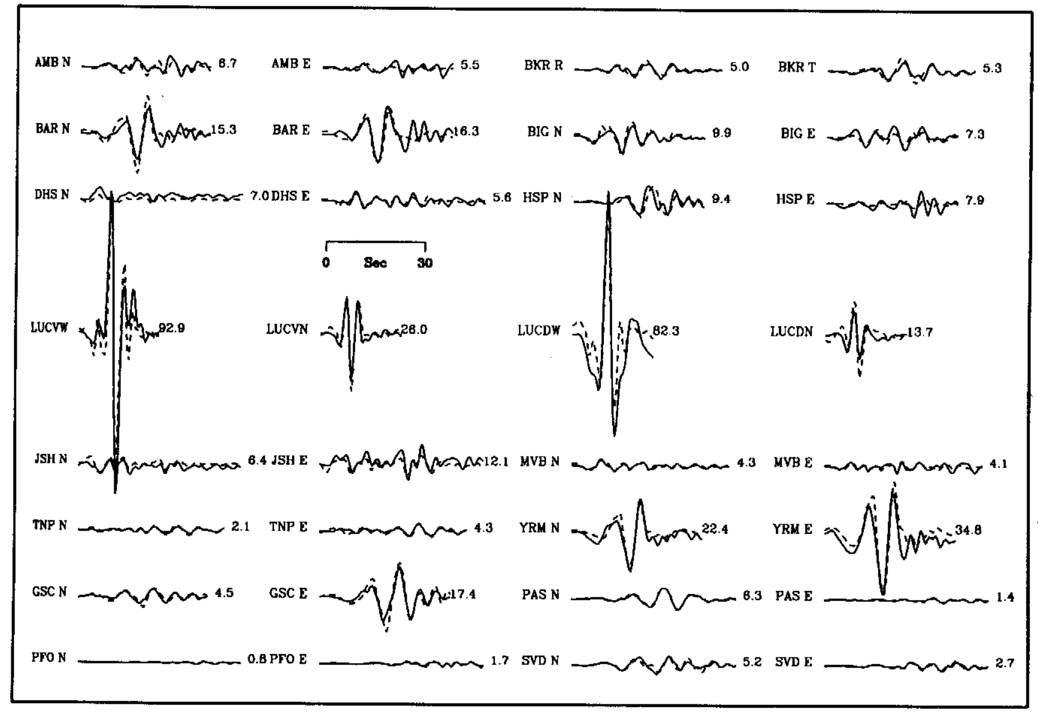

Figure 11. Strong-motion displacement observations (solid lines) and synthetics (dashed lines) for the strong-motion dislocation model. Observed amplitudes are given to the right of each trace in centimeter, and all have a common scale. For station LUC (Lucerne Valley), both velocity (LUCVW, LUCVN) and displacement (LUCDW, LUCDN) data and synthetics are presented, with the velocity amplitudes in cm/sec.

Variability

Wald et Heaton, 1994

Damage map during the 1976 Guatemala earthquake.

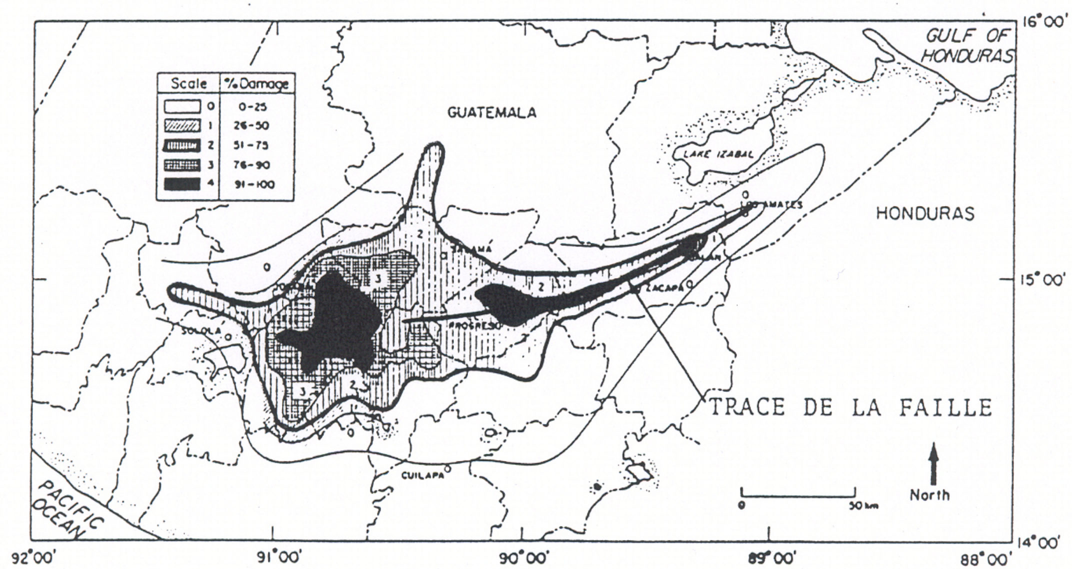

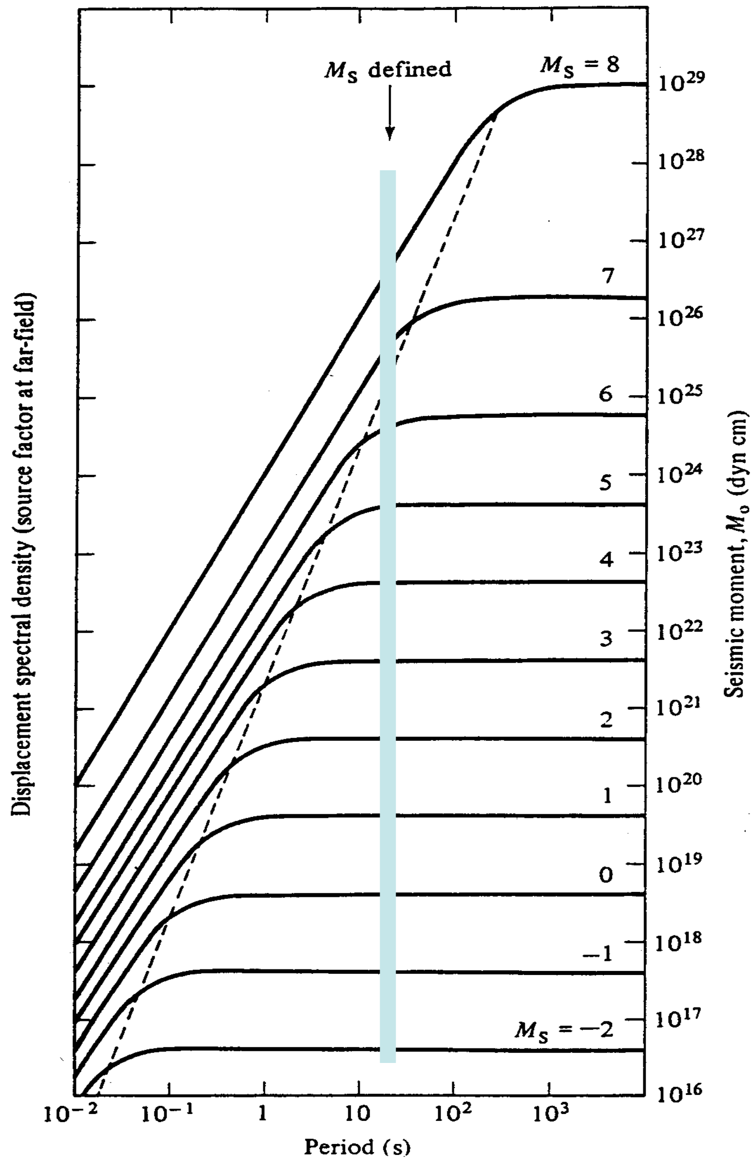

Biais of 'instrumental' magnitude

Aki, 1967